

# Automatic Segmentation of Neonatal Brain MRI

<sup>1</sup>Marcel Prastawa, <sup>2</sup>John Gilmore, <sup>3</sup>Weili Lin, and <sup>1,2</sup>Guido Gerig

Department of <sup>1</sup>Computer Science, <sup>2</sup>Psychiatry, and <sup>3</sup>Radiology  
University of North Carolina, Chapel Hill, NC 27599, USA  
`prastawa@cs.unc.edu` \*

**Abstract.** This paper describes an automatic tissue segmentation method for neonatal MRI. The analysis and study of neonatal brain MRI is of great interest due to its potential for studying early growth patterns and morphologic change in neurodevelopmental disorders. Automatic segmentation of these images is a challenging task mainly due to the low intensity contrast and the non-uniformity of white matter intensities, where white matter can be divided into early myelination regions and non-myelinated regions. The degree of myelination is a fractional voxel property that represents regional changes of white matter as a function of age. Our method makes use of a registered probabilistic brain atlas to select training samples and to be used as a spatial prior. The method first uses graph clustering and robust estimation to estimate the initial intensity distributions. The estimates are then used together with the spatial priors to perform bias correction. Finally, the method refines the segmentation using sample pruning and non-parametric density estimation. Preliminary results show that the method is able to segment the major brain structures, identifying early myelination regions and non-myelinated regions.

## 1 Introduction

Magnetic resonance imaging is the preferred imaging modality for in vivo studies of brain structures of neonates. Potential applications include the analysis of normal growth patterns and the study of children at high risk for developing schizophrenia and other neurodevelopmental disorders. This typically involves the reliable and efficient processing of a large number of datasets. Therefore, automatic segmentation of the relevant structures from neonatal brain MRI is critical. This task is considerably more difficult when compared with the segmentation of brain MRI of infants and adults. This is due to a number of factors: low contrast to noise ratio, intensity inhomogeneity (bias field), and the inhomogeneity of the white matter structure. White matter is separated into myelinated white matter and non-myelinated white matter, often with ambiguous boundaries and as a regional pattern that changes with age.

---

\* This research is supported by the UNC Neurodevelopmental Disorders Research Center (PI Joseph Piven) HD 03110 and the NIH Conte Center MH064065. Marcel Prastawa is supported by R01 HL69808 NIH-NCI (PI E. Bullitt).

Experience shows that automatic segmentation methods for healthy adult brain MRI generally fail to properly segment neonatal brain MRI. However, the concepts and approaches for segmenting adult brains are still applicable for neonatal brains if adjusted to tackle the specific problems. Matsuzawa *et al.* [1] showed neonatal brain segmentation from MRI as a part of a study of early brain development. The results show that the method has difficulties dealing with tissue separation. The segmentations of one-month-old infants show mostly noise, although axial MRI slices visually leave the impression that there are intensity differences between non-myelinated white matter and gray matter. Most advanced work has been demonstrated by Warfield *et al.* [2,3], but subjects were mostly preterm babies presenting less complex cortical folding.

A successful concept for robust, automatic tissue segmentation of adult brains is to use the information provided by a brain atlas. The brain atlas can be used as spatial priors for segmentation [4,5]. The template-moderated segmentation proposed by Warfield *et al.* [6] clearly demonstrates the strength of the use of a spatial prior since regions that overlap in intensity space but are spatially disjoint can be separated. However, there is no spatial model for early myelination regions in white matter since this is an infiltrating tissue property. Cocosco *et al.* [7] demonstrated automatic, robust selection of training samples for different tissue categories using only regions with high atlas probabilities. Additionally, this research proposed non-parametric clustering to overcome limitations of traditional mixture Gaussian models. Brain tissue segmentation based on fractional voxel properties has been developed by Shattuck *et al.* [8], motivated by the need to improved tissue segmentation in the presence of pathological regional changes. Preliminary feasibility tests with our 3 Tesla neonatal MRI with the EMS method [5] were shown in Gerig *et al.* [9].

We have developed a new atlas based segmentation method for neonatal brain MR images. The atlas is used as a guide to determine sample locations and also defines spatial prior probabilities for tissue to improve robustness of classification. Incorporating spatial priors into the process is essential for separating different tissues that have low contrast. Our method combines the graph clustering approach by Cocosco *et al.* [7], the bias correction scheme by Van Leemput *et al.* [10], and the robust estimation algorithm by Rousseeuw *et al.* [11]. In contrast to most other brain segmentation schemes, our new segmentation method integrates bias correction, non-parametric classification, and brain masking into one method.

## 2 Method

Unlike in adult brains, white matter in neonatal brains cannot be treated as a single structure. White matter is composed of large non-myelinated regions and small regions of early myelination (mostly seen in the internal capsule and along the projection tracts towards the motor cortex). Non-myelinated white matter in infants have the inverse intensity properties as compared to adult white matter, it is dark in T1-weighted images and bright in T2-weighted images. Early

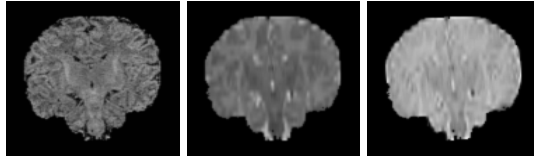


**Fig. 1.** Example neonatal MRI dataset with early myelination: the filtered and bias corrected Neonate-0026 dataset. From left to right: T1-weighted image, T2-weighted image, and the proton density image.

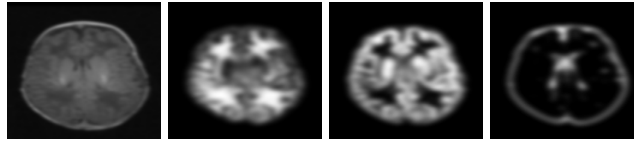


**Fig. 2.** The neonatal brain atlas-template created from a single subject segmentation and blurring. From left to right: T1 template image, white matter (both myelinated and non-myelinated), gray matter, and cerebrospinal fluid probabilities.

myelination in white matter is shown as hyper intense regions in T1-weighted images and hypo intense regions in T2-weighted images. Fig. 1 shows an example of neonatal brain MRI in different modalities with early myelination regions.

Due to the different growth patterns across subjects and significant changes over the first few months of development, it would be difficult to obtain separate spatial models for the two different white matter classes. Therefore, we use a single spatial prior for white matter that provides the probability for every voxel to be either a myelinated white matter or non-myelinated white matter. Spatial and geometric differences between the two classes are difficult to summarize, so the identification of the different white matter classes is set to be driven by image intensities. To test our method, we have created a template atlas shown in Fig. 2. The template atlas was created from the segmentation of one dataset that was done using a semi-automatic segmentation method. The human rater first removes the skull and background using thresholding and user-supervised level set evolution. The rater then manually marks regions for each tissue type in different areas throughout the brain. From the user-selected regions, a bias field estimate is extrapolated and then used to correct the inhomogeneity. The segmentation is obtained using the k-nearest neighbor algorithm using training samples from the selected regions. The segmentation result is then edited manually to correct for possible errors. We then blur the final segmentation result to simulate the population variability. The creation of a brain atlas that sufficiently describes the true variability of the population is a significant challenge beyond the scope of this paper, but is currently in progress.

The segmentation process is initialized by registering the subject to the atlas using affine transformation and the mutual information image match metric [12].

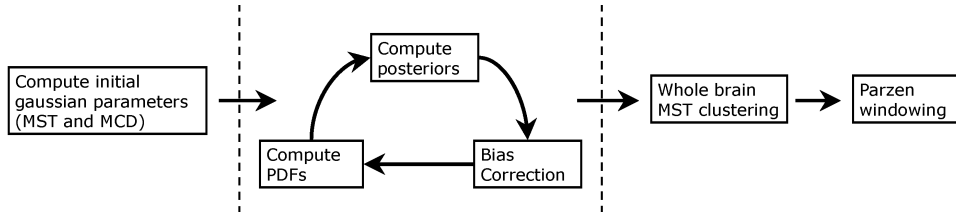


**Fig. 3.** Overview of the segmentation algorithm. The dashed lines show the division of the process to three major steps: initial estimation of parameters using MCD and MST clustering, bias correction, and refinement using a non-parametric segmentation method.

The registered images are then filtered using anisotropic diffusion [13]. Since the relative ordering of the different structures are known, the clustering method using the Minimum Spanning Tree (MST) proposed by Cocosco *et al.* [7] is ideal. However, this method requires that the input images are already bias corrected and that the brain regions are identified. These tasks are not easily accomplished given the intensity properties of neonatal MRI. Our method combines the clustering method with robust estimation and bias correction using spatial probabilities. The method is composed of three major steps, as shown in Fig. 3. First, it obtains rough estimates of the intensity distributions of each tissue class. It then iteratively performs segmentation and bias correction. Finally, it refines the segmentation result using a non-parametric method.

## 2.1 Estimation of Initial Gaussian Parameters

The first step in the segmentation process determines the rough estimates of the intensity distributions. Here, we choose to use the Gaussian as a rough model of the intensity distributions. The parameters for the multivariate Gaussians are computed through the combination of the Minimum Covariance Determinant (MCD) estimator and MST edge breaking to the training samples.

The training samples are obtained by selecting a subset of the voxels with high probability values (ex.  $\tau > 0.9$ ). Additionally, we use the image gradient magnitudes as a sampling constraint. The 2-norm of the image gradient magnitudes at voxel location  $x$ ,  $G(x) = \sqrt{|\nabla I_1(x)|^2 + \dots + |\nabla I_n(x)|^2}$ , is the measure we have chosen. Samples with  $G(x)$  greater than the average  $G(x)$  over the candidate white matter regions ( $Pr(wm) > 0$ ) is removed to avoid sampling in the transition regions between myelinated and non-myelinated white matter and at white/gray matter boundaries. The removal of samples from the partial volume regions aids the clustering process (Fig. 4).

Once the samples are obtained, we compute the initial parameters for gray matter and csf using the robust mean and covariance from the MCD estimator [11]. The result of the MCD algorithm is the ellipsoid that covers at least half of the data with the smallest determinant of covariance. We then apply

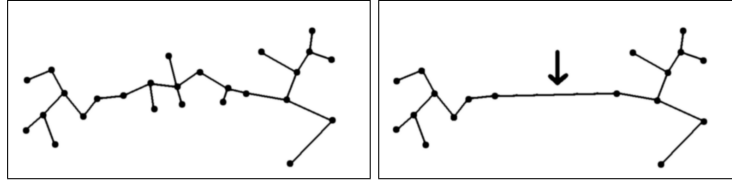


**Fig. 4.** Illustrations of the Minimum Spanning Trees for white matter obtained using different sampling strategies. Left: Samples with high probability values. Right: Samples with high probability values and low gradient magnitude. Choosing only samples with low gradient magnitude helps to remove samples from the transition regions between myelinated white matter and non-myelinated white matter and gray/white boundary voxels. This is crucial for clustering based on edge breaking. As seen on the right picture, breaking the longest edge marked by the arrow would give two well separated clusters.

the graph clustering method through MST edge breaking to the white matter samples. The two white matter distributions are computed using an iterative process similar to the one described in [7]:

1. Given a threshold value  $T$ , break edges incident with node  $i$  that have length greater than  $T \times A(i)$ , where  $A(i)$  is the average length of all edges incident on node  $i$ .
2. Determine the two largest clusters and their means using the MCD algorithm. The two clusters are sorted based on the robust mean along one of the intensity features (set the first cluster to represent early myelination).
3. Stop when the two clusters satisfy the relative ordering criterion along one of the intensity features. For example, the robust mean values for the T2 intensity feature must follow the relation:  $\mu_{myel} < \mu_{gm} < \mu_{non-myel} < \mu_{csf}$
4. Otherwise, decrease the value of  $T$  and go back to step 1.

Once the two white matter clusters are identified, the robust mean and covariance of the two clusters obtained through the MCD algorithm is used as the initial Gaussian distributions for white matter. The initial Gaussian parameters are then combined with spatial priors in the next step where this initial segmentation is used to estimate the bias field.

## 2.2 Bias Correction

Neonatal brain MR images exhibit higher intensity variability for each tissue and low intensity contrast as compared to adult MRI. These two factors severely hamper the estimation of intensity inhomogeneity. We have experimented with a histogram based intensity inhomogeneity correction, developed by Styner *et al.* [14]. We concluded that histogram based method would often fail to obtain the optimal solution. The histogram of a neonatal brain MR dataset is generally smooth with weak maximas.

In the case of bias correction of neonatal brain MRI, the spatial context is useful to deal with the low intensity contrast. We have chosen to use the method developed by Van Leemput *et al.* [10]. The bias correction scheme uses the spatial probabilities to estimate the bias field. The bias field is estimated by fitting a polynomial to the log difference between the original image and the reconstructed homogeneous image.

### 2.3 Segmentation Refinement

At this stage, the images are already bias corrected and the brain regions are identified. However, the Gaussian does not seem the optimal model for the intensity distributions due to large intensity variability. Therefore, segmentation obtained using this model generally has more false positives. In order to refine the segmentation results, we apply the MST clustering method [7] to prune the samples. Instead of using probability thresholding, we simply use the previous classification labels for sample selection. The training samples obtained using this method is then used to estimate the probability density functions of each class using Parzen windowing or kernel expansion.

## 3 Results

We have applied the method to two cases, as shown in Fig. 5. Visual inspection shows that the major regions are properly identified, although the distinction between myelinated white matter and non-myelinated white matter is incorrect in some regions. The myelinated white matter regions are mostly distributed near the spine (central posterior). We also observed the presence of myelinated white matter around the regions associated with the sensory and motor cortex.

Quantitative validation of the segmentation results is inherently difficult due to the lack of a gold standard. The common standard, comparison with manual segmentations, does not seem to be feasible since highly convoluted structures in low-contrast, noisy data are hard to trace. In addition to that, the myelinated white matter and the non-myelinated white matter have ambiguous boundaries, which would make manual segmentation results highly variable and difficult to reproduce. This problem is solved for adult brains by offering web-based archives with simulated datasets [15] and manually segmented real datasets<sup>1</sup>. We are currently working on contour-based segmentation with subsequent manual interaction to provide standardize test data for validation. .

## 4 Discussion and Conclusion

Efficient and robust segmentation of tissue and degree of myelination would have a large impact in neonatal MRI studies, because early detection of pathology may permit early intervention and therapy. Neonatal brain MRI offers unique

---

<sup>1</sup> Internet Brain Segmentation Repository, <http://www.cma.mgh.harvard.edu/ibsr>

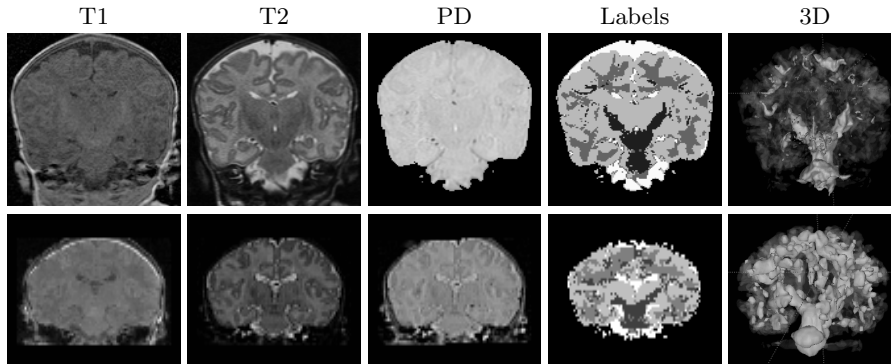


**Fig. 5.** The datasets and the generated segmentation results (top: high quality dataset provided by Petra Hüppi, bottom: Twin-0001A dataset). The results show that our method identifies the major brain structures, including the early myelination regions and the non-myelinated white matter regions. The classification labels are encoded as gray values, from darkest to brightest: myelinated white matter, non-myelinated white matter, gray matter, and csf. The 3D images show the segmented myelinated white matter (solid) and non-myelinated white matter (transparent).

challenges for image analysis. Standard automated segmentation methods fail as there is reduced contrast between white and gray matter in neonates. Noise is larger since non-sedated neonates need to be scanned with a high-speed MRI protocol to avoid motion artifacts. White matter is also heterogeneous, with hyper intense myelinated white matter (in T1 image) compared to non-myelinated white matter. The low contrast and visible contours in the data suggest that a boundary-based approach would be ideal as opposed to voxel-by-voxel statistical pattern recognition. Tissue segmentation by statistical pattern recognition on voxel intensities by definition lacks the concept of finding boundaries. On the other hand, the poor quality of the data and high complexity of convoluted structures presents a challenge for boundary driven segmentation methods.

We have presented an atlas-based automatic segmentation method for multi-channel neonatal MRI data. The method uses graph clustering and robust estimation to obtain good initial estimates, which are then used to segment and correct the intensity inhomogeneity inherent in the image. The segmentation is then refined through the use of a non-parametric method. Visual inspection of the results shows that the major structures are properly segmented, while the separation of myelinated and non-myelinated white matter still lacks spatial coherence in some regions. The availability of a real neonatal probabilistic brain atlas that captures the variability of the population is a critical issue for the proposed method. The creation of such an atlas requires the segmentation of a set of representative datasets and may require deformable registration for reducing the high shape variability, which make the task highly challenging.

## Acknowledgements

We acknowledge Petra Hüppi for providing a high quality neonate dataset, Koen Van Leemput for providing the MATLAB code that aids the development of the bias correction software, and the ITK community (<http://www.itk.org>) for providing the software framework for the segmentation algorithm.

## References

1. Matsuzawa, J., Matsui, M., Konishi, T., Noguchi, K., Gur, R., Bilder, W., Miyawaki, T.: Age-related volumetric changes of brain gray and white matter in healthy infants and children. *Cerebral Cortex* **11** (2001) 335–342
2. Warfield, S.K., Kaus, M., Jolesz, F.A., Kikinis, R.: Adaptive, template moderated, spatially varying statistical classification. *Med Image Anal* **4** (2000) 43–55
3. Hüppi, P., Warfield, S., Kikinis, R., Barnes, P., Zientara, G., Jolesz, F., Tsuji, M., Volpe, J.: Quantitative magnetic resonance imaging of brain development in premature and normal newborns. *Ann Neurol* **43** (1998) 224–235
4. Wells, W.M., Kikinis, R., Grimson, W.E.L., Jolesz, F.: Adaptive segmentation of MRI data. *IEEE TMI* **15** (1996) 429–442
5. Van Leemput, K., Maes, F., Vandermeulen, D., Suetens, P.: Automated model-based tissue classification of MR images of the brain. *IEEE TMI* **18** (1999) 897–908
6. Warfield, S., Dengler, J., Zaers, J., Guttman, C., Wells, W., Ettinger, G., Hiller, J., Kikinis, R.: Automatic identification of gray matter structures from MRI to improve the segmentation of white matter lesions. *Journal of Image Guided Surgery* **1** (1995) 326–338
7. Cocosco, C.A., Zijdenbos, A.P., Evans, A.C.: A fully automatic and robust brain MRI tissue classification method. *Medical Image Analysis* **7** (2003) 513–527
8. Shattuck, D.W., Sandor-Leahy, S.R., Schaper, K.A., Rottenberg, D.A., Leahy, R.M.: Magnetic resonance image tissue classification using a partial volume model. *NeuroImage* **13** (2001) 856–876
9. Gerig, G., Prastawa, M., Lin, W., Gilmore, J.: Assessing early brain development in neonates by segmentation of high-resolution 3T MRI. In: MICCAI. Number 2879 in LNCS, Springer (2003) 979–980 Short Paper.
10. Van Leemput, K., Maes, F., Vandermeulen, D., Suetens, P.: Automated model-based bias field correction of MR images of the brain. *IEEE TMI* **18** (1999) 885–896
11. Rousseeuw, P.J., Van Driessen, K.: A fast algorithm for the minimum covariance determinant estimator. *Technometrics* **41** (1999) 212–223
12. Maes, F., Collignon, A., Vandermeulen, D., Marchal, G., Suetens, P.: Multimodality image registration by maximization of mutual information. *IEEE TMI* **16** (1997) 187–198
13. Gerig, G., Kübler, O., Kikinis, R., Jolesz, F.: Nonlinear anisotropic filtering of MRI data. *IEEE TMI* **11** (1992) 221–232
14. Styner, M., Brechbuhler, C., Szekeley, G., Gerig, G.: Parametric estimate of intensity inhomogeneities applied to MRI. *IEEE TMI* **19** (2000) 153–165
15. Collins, D.L., Zijdenbos, A.P., Kollokian, V., Sled, J.G., Kabani, N.J., Holmes, C.J., Evans, A.C.: Design and construction of a realistic digital brain phantom. *IEEE TMI* **17** (1998) 463–468